

Dual ABCA4-AAV Vector Treatment Reduces Pathogenic Retinal A2E Accumulation in a Mouse Model of Autosomal Recessive Stargardt Disease

Frank M. Dyka,^{1,*} Laurie L. Molday,² Vince A. Chiodo,¹
Robert S. Molday,^{2,3} and William W. Hauswirth¹

¹Department of Ophthalmology, College of Medicine, University of Florida, Gainesville, Florida; Departments of ²Biochemistry and Molecular Biology and ³Ophthalmology and Visual Sciences, University of British Columbia, Vancouver, British Columbia, Canada.

Autosomal recessive Stargardt disease is the most common inherited macular degeneration in humans. It is caused by mutations in the retina-specific ATP binding cassette transporter A4 (ABCA4) that is essential for the clearance of all-*trans*-retinal from photoreceptor cells. Loss of this function results in the accumulation of toxic bisretinoids in the outer segment disk membranes and their subsequent transfer into adjacent retinal pigment epithelium (RPE) cells. This ultimately leads to the Stargardt disease phenotype of increased retinal autofluorescence and progressive RPE and photoreceptor cell loss. Adeno-associated virus (AAV) vectors have been widely used in gene therapeutic applications, but their limited cDNA packaging capacity of ~4.5 kb has impeded their use for transgenes exceeding this limit. AAV dual vectors were developed to overcome this size restriction. In this study, we have evaluated the *in vitro* expression of ABCA4 using three options: overlap, transplicing, and hybrid ABCA4 dual vector systems. The hybrid system was the most efficient of these dual vector alternatives and used to express the full-length ABCA4 in *Abca4*^{-/-} mice. The full-length ABCA4 protein correctly localized to photoreceptor outer segments. Moreover, treatment of *Abca4*^{-/-} mice with this ABCA4 hybrid dual vector system resulted in a reduced accumulation of the lipofuscin/N-retinylidene-N-retinylethanolamine (A2E) autofluorescence *in vivo*, and retinal A2E quantification supported these findings. These results show that the hybrid AAV dual vector option is both safe and therapeutic in mice, and the delivered *ABCA4* transgene is functional and has a significant effect on reducing A2E accumulation in the *Abca4*^{-/-} mouse model of Stargardt disease.

Keywords: AAV dual vectors, Stargardt disease, AAV hybrid vectors

INTRODUCTION

STARGARDT DISEASE (STGD1; MIM #248200) IS the most common autosomal recessive form of early onset macular dystrophy with an overall prevalence of 1:8,000–10,000.¹ The disease is characterized by a loss of retinal pigment epithelium (RPE) cells and photoreceptors and, as a consequence, results in a progressive loss of central vision and visual acuity throughout life, usually beginning in the first or second decade of life. The most common form of Stargardt disease is caused by mutations in the ATP binding cassette transporter A4 (*ABCA4*) gene, which functions in photoreceptor outer segments.²

ABCA4 is a lipid transporter localized primarily to the rim region of rod and cone photoreceptor outer segment disks although low level expression in photoreceptor inner segments and the endolysosomes of the RPE has also been reported.^{3–6} The protein consists of two nonidentical halves, each containing a large extracellular domain protruding into the disk lumen, six transmembrane domains, and an intracellular domain with a nucleotide-binding domain.⁷ ABCA4 is critically important for the clearance of photoisomerized all-*trans*-retinal from the photoreceptor disk lumen. The preferred substrate for transport is N-retinylidene-phosphatidylethanolamine (N-ret-PE),

*Correspondence: Dr. Frank M. Dyka, Department of Ophthalmology, College of Medicine, University of Florida, 1600 SW Archer Road, ARB R1-236, Gainesville, FL 32610. E-mail: fmdyka@ufl.edu

a spontaneous condensation product of all-*trans*-retinal with phosphatidylethanolamine.⁸ ABCA4 flips the N-ret-PE from the luminal leaflet of the disks to the cytosolic leaflet from where it is reduced by the action of RDH8⁹ and transported to the RPE for recycling of the photopigment back to its 11-*cis* configuration. Loss of ABCA4 function leads to toxic accumulation of bisretinoids, specifically N-retinylidene-N-retinylethanolamine (A2E), a condensation product of all-*trans*-retinal with N-ret-PE in the outer segments. It is the major fluorescent compound of Stargardt lipofuscin aggregates.^{10–12} This fluorescence emanates from the RPE after ingestion of photoreceptor outer segment tips and is a key indicator for the early clinical diagnosis of Stargardt disease in humans.¹³ As a recessive monogenic disease with a well-described genotype–phenotype relationship, ABCA4-Stargardt presents as an excellent target for gene supplementation therapy.

Adeno-associated virus (AAV) has shown proven potential for gene therapy in the retina. It has demonstrated efficacy and safety in proof-of-concept studies and in clinical trials,^{14–25} and recently the first retinal gene therapy in the United States was approved and employed an AAV vector.²⁶ Upon target cell entry, AAV genomes persist as episomal DNA in the nucleus, a stable condition in postmitotic cells. The major limitation of AAV is its small payload capacity of ~4.5 kb. Although it was initially reported that an entire oversized transgene could be encapsulated in an AAV capsid,²⁷ it was later shown that packaging of such oversized transgene cassettes results in random truncations/deletions of the DNA during the vector packaging process.^{28–33} These fragmented genomes undergo homologous recombination after transduction of cells, which ultimately leads to the expression of protein. Compared with vectors with cDNAs <4.5 kb, the packaging of oversized cDNAs into AAV vectors is highly inefficient, resulting in low vector titers, and its transduction efficiency of target cells is poor.^{28,29} Critically, the sequence randomness of the packaged DNA makes it impossible to characterize their precise composition after vector production, a necessary prerequisite for clinical applications. In addition, these sorts of fragmented transgenes present the clear risk of imperfect reconstitution of the normal coding sequence upon exposure to the cellular DNA double-strand break repair machinery.³³

To overcome these drawbacks for cDNAs exceeding the size limit of AAV vectors, dual vector strategies for oversized transgenes have been developed in which the oversized transgene cassette

is split between two discreet vectors.^{25,34–43} One vector contains a promoter and the 5′ portion of the cDNA and the other vector contains the 3′ portion of the cDNA and the polyadenylation signal (polyA). After coinfection, intermolecular concatemerization mediated through overlapping elements or the vector inverted terminal repeats (ITRs) ultimately lead to expression of the full-length protein.^{44,45} Several improvements over the original dual vector platforms have been developed utilizing highly recombinogenic sequences shared between 5′ and 3′ vector or oligonucleotides to tether 5′ and 3′ vectors together.^{35,42,46,47}

In this study, we examine the potential of three principal AAV dual vector systems for a gene supplementation therapy for Stargardt disease and show the best performing system has the ability to express ABCA4 *in vitro* and *in vivo* and lead to therapeutic reduction of A2E in a mouse model.

MATERIALS AND METHODS

Cloning

Three AAV dual vector platforms were created for this study. The principal arrangement of elements is shown in Fig. 1. In short, to create the overlap dual vector platform (Fig. 1B), the 5′ and 3′ portions of ABCA4 were amplified by PCR with Pfu-Turbo polymerase (Agilent Technologies, Santa Clara, CA) using primers P1/P2 and P3/P4, respectively. Restriction sites were introduced through the primers for cloning purposes (Table 1). The PCR products were treated with the respective restriction endonucleases (New England Biolabs [NEB], Ipswich, MA) and cloned into vectors described in a previous publication,³⁶ replacing the myosin VIIa coding sequence. The overlap platforms B2 and B3 were generated by digesting vector B1 with *NotI/BamHI* and *NotI/FseI* followed by blunt ending these restriction fragments with T4 DNA polymerase (NEB) and ligation with T4 DNA Ligase (NEB) according to the manufacturer's instructions. To create the transplating vector platform (Fig. 1C), fragments of the ABCA4 sequence were amplified with primers P5/P6 and P7/P8, introducing splice donor and acceptor sites. The hybrid vector platform (Fig. 1D) was created by adding a highly recombinogenic element derived from the alkaline phosphatase gene (AP)^{42,48} to the transplating vector platform utilizing primers P9/P10 and P11/P12. All constructs were sequence verified by Sanger sequencing (University of Florida ICBR Sequencing Core, Gainesville, FL).

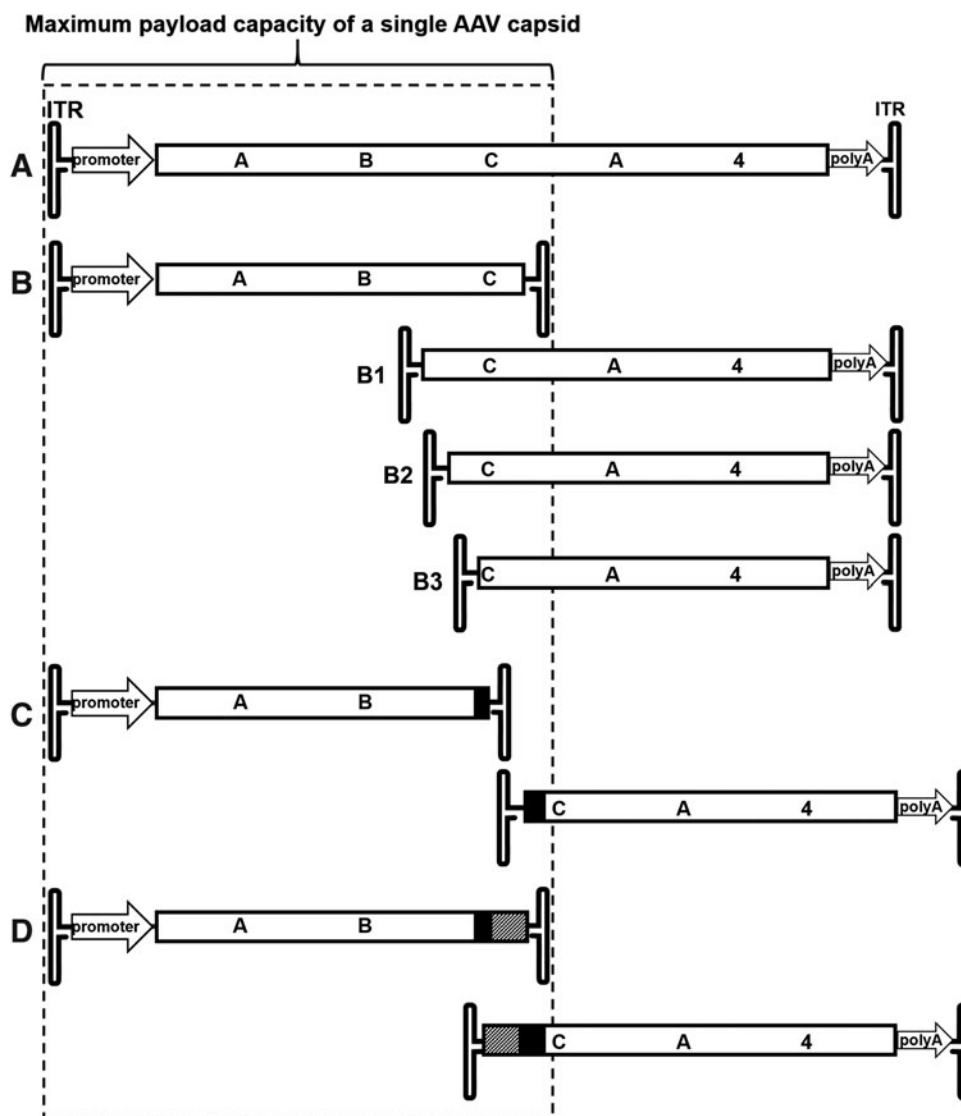


Figure 1. Schematic of ABCA4 dual AAV vector platforms created for this study. **(A)** Full-length ABCA4 expression cassette. **(B)** Overlap vector showing the three overlaps tested (B1–B3). **(C)** Transposing vector. **(D)** Hybrid vector platform. Promoter, cytomegalovirus immediate early/chicken β -actin chimeric promoter; ITR, inverted terminal repeat; polyA, polyadenylation signal; splice donor/acceptor sites marked *black* regions; AP overlap sequences marked as *hatched* regions. AAV, adeno-associated virus; ABCA4, ATP binding cassette transporter A4; AP, alkaline phosphatase.

AAV vector production

The vectors were packaged in AAV2 capsids for *in vitro* analyses. Vectors for *in vivo* analyses were packaged in AAV8(Y733F) capsids.⁴⁹ All vectors were packaged and purified by standard methods as previously described.^{50,51}

Infections

Human embryonic kidney (HEK293) cells were seeded into six-well cell culture plates. Infections with dual AAV vector pairs were then performed in HEK293 cells as well. In brief, cells were grown to 60–70% confluency and the vectors were diluted in balanced salt solution to the desired multiplicity of infection (MOI). If not otherwise mentioned, in-

fections were carried out at 10,000 particles/cell of each vector, resulting in an MOI of 20,000 particles/cell total for each vector pair. Cells were incubated in 10% serum containing media for 3 days postinfection at 37°C under 7% CO₂ and were then analyzed through immunoblotting (details hereunder). Cells transfected with the full-length cDNA on a single plasmid were used as a positive control for immunoblot analyses to highlight the correct size of the full-length ABCA4 protein.

Animals

Vectors were injected subretinally into 4-week-old 129S-Abca4^{tm1Ght}/J mice (Jackson Laboratory, Bar Harbor, ME). Animals were maintained under

Table 1. Oligonucleotide primers used to construct the ATP binding cassette transporter A4 dual vectors platforms

Overlap Vectors		
P1	GCGGCGGCGCCACCATGGGCTTCGTGAGACAG	<i>NotI</i>
P2	GCGACTAGTGTGGCATATGCTCTGTGC	<i>SpeI</i>
P3	GCGGCGGCGCGCTTACTGTCTCCGGTGGC	<i>NotI</i>
P4	GCGGAGCTCTCAGTCTGGGCTTGTGC	<i>SacI</i>
Transsplicing Vectors		
P5	AGATTTTGGAGCCCTGTGGC	(<i>FseI</i>)
P6	CTGCACTAGTGTGACAGAAACGCAAGAGTCTTCTGTCTCGACA AGCCAGTTTCTATTGGTCTCTTAAACCTGTCTGTAACCTTGA TACTTACCTGATAGGTCCTGAGCCTC	<i>Sall</i>
P7	GACTGGCGGCGCTCGCGATAGGCACCTATTGGTCTTACTGACATC CACTTTGGCTTTCTCTCCACAGGTGGCATGCAGAGAAAGCTG	<i>NotI</i>
P8	TGTTGTCTTCAGTTTCTAGATG	<i>XbaI</i>
Hybrid Vectors		
P9	GCTTGGTTCGACGAAACGGTCCAGGCTATGTG	<i>Sall</i>
P10	GCTTGGTTCGACCCCGGGTGC GCGGCGG	<i>Sall</i>
P11	CGTTCCGCGGCGCCCGGGTGC GCGGCGG	<i>NotI</i>
P12	CGTTCCGCGGCGGAAACGGTCCAGGCTATGTG	<i>NotI</i>

The restriction sites introduced through the primers are listed and underlined in the sequence (The *FseI* site is only partially contained in primer P5).

standard laboratory conditions (18–23°C, 40% to 65% humidity) with food and water available *ad libitum* on a 12/12 h light (200 lux) dark cycle in the University of Florida Health Science Center's animal care facilities and were handled in accordance with the ARVO statement for Use of Animals in Ophthalmic and Vision Research and the guidelines of the Institutional Animal Care and Use Committee of the University of Florida.

Subretinal injections

One microliter of ABCA4 AAV8(Y733F) hybrid dual vector pairs was injected subretinally into one eye of 129S-Abca4^{tm1Ght/J} mice (Jackson Laboratory). Subretinal injections were performed as previously described.⁵² In brief, mouse eyes were dilated with 2.5% phenylephrine (Paragon Biotek, Portland, OR) and 1% atropine (Akorn, Lake Forest, IL). Mice were anesthetized with 100 mg/kg ketamine and 8 mg/kg xylazine. An incision in the peripheral cornea was made with a 30-gauge needle under a surgical stereomicroscope, followed by insertion of a blunt-tip 33-gauge needle on a Hamilton syringe. The retina was then punctured with the blunt needle and the 1 μ L content of the syringe, either AAV vectors or buffer, was slowly injected into the subretinal space creating a temporary retinal detachment. Mice were kept on a 37°C heating pad during injection and recovery after anesthesia. Further analysis was carried out only on animals that received comparable successful injections. Eyes exhibiting significant damage or

hemorrhage by fundus visualization or optical coherence tomography were excluded from further analysis. Two animals each in the experimental and the control group showed a permanent retinal detachment in the injected eye. In addition, in the experimental group, one mouse exhibited strong retinal bleeding upon injection and two mice developed cataract in both eyes. This resulted in 22 and 9 successful injected animals in the experimental and control group, respectively. During the course of the experiment, one animal in each group did not recover from anesthesia.

Fundus autofluorescence

Fundus autofluorescence accumulation in mice was measured with a confocal scanning laser ophthalmoscope (cSLO; Heidelberg Engineering, Heidelberg, Germany). Mice were dilated with tropicamide (Akorn), anesthetized with ketamine/xylazine and positioned on a platform. Measurement of autofluorescence was done as described elsewhere.⁵³ In brief, a drop of lubricant eye drops (GenTeal; Alcon, Fort Worth, TX) was applied to each eye and contact lenses were carefully placed and centered, avoiding air bubbles. The camera was positioned in infrared mode for maximal illumination of the inside of the eye, and the focus was adjusted to the point of maximal reflectance, which generally is the RPE layer in pigmented animals. The mode was then switched to fundus angiography to record 488 nm autofluorescence and the camera repositioned for maximal illumination if necessary. Photopigments were bleached for 1 min before measuring fundus autofluorescence with normalization off. Recorded pictures were exported into ImageJ and the grayscale value of the A2E signal was quantified by drawing an annular ring around the optic nerve disk utilizing the "make band" function. Individual background signals were subtracted from each measurement and the resulting background-corrected gray scale value was used for statistical analysis.

A2E quantification

Quantification of A2E was carried out as previously described.^{6,54} In brief, two to four posterior eye cups from treated or untreated Abca4^{-/-} mice were pooled and homogenized in phosphate buffer. An equal volume of two parts chloroform and one part methanol was added to each sample. The organic phases from three such extractions were then pooled and dried under argon. The sample was then dissolved in methanol containing 0.1% trifluoroacetic acid (TFA). High-performance liquid chromatography (HPLC) analysis (Hewlett

Packard 1100 Series HPLC; Agilent Technologies) was performed using a reverse phase C18 column and a 90% to 100% gradient of acetonitrile in water containing TFA followed by 100% acetonitrile. A2E was monitored at 430 nm and confirmed by spectral analysis as previously described.⁵⁵ The amount of A2E was determined in relation to an external A2E standard.

Protein extraction and immunoblotting

Transfected and infected HEK293 cells were harvested and washed twice in phosphate-buffered saline (PBS) (137 mM NaCl, 2.7 mM KCl, 10 mM Na₂HPO₄, and 1.8 mM KH₂PO₄). The final pellet was resuspended in 100 μ L of PBS and added to an equal volume of PBS containing 2% Triton X-100, and complete protease inhibitor (Roche Applied Science). After 1 h at 4°C, the solution was centrifuged at 20,000 *g* for 10 min and the supernatant was retained for SDS gel electrophoresis. The protein concentration of the supernatant was measured with BCA (Thermo Fisher Scientific, Rockland, IL). Equal amounts of protein were denatured in Laemmli buffer (BioRad, Hercules, CA) containing 4% 2-mercaptoethanol and separated on 4–20% SDS-PAGE gels (BioRad) and transferred in Tris-glycine buffer (25 mM Tris, 192 mM glycine, pH 8.3) containing 5% methanol onto polyvinylidene fluoride membranes (Millipore, Billerica, MA). Blots were blocked with 1 \times blocking buffer (Li-Cor, Lincoln, NE) and labeled with antibodies against ABCA4, rim3F4, or rim5B4,^{5,56} and beta-actin (ab 34731, 1:5000; Abcam, Cambridge, MA) for 1 h. For visualization with the Odyssey system (Li-Cor), an antimouse and an antirabbit secondary antibody conjugated with CW800 and IR680 dyes (Li-Cor), respectively, were used.

Tissue processing and immunohistochemistry

Six weeks postinjection, 129S-Abca4^{tm1Ght}/J mice were enucleated and their eyes processed and immunostained as previously described with minor modifications.⁵⁷ The retinas were stained with the ABCA4-specific antibody rim5B4. Images were obtained with a spinning disk confocal microscope (Nikon Eclipse TE2000 microscope equipped with Perkin Elmer Ultraview Modular Laser System and Hamamatsu O-RCA-R2 camera) using 20 \times (air) objective lenses. Image analysis was performed using Volocity 5.5 software (Perkin Elmer, Waltham, MA).

Statistical analysis

Statistical differences between groups were assessed by an unpaired *t*-test (GraphPad Prism 6.0;

GraphPad Software, San Diego, CA). Error bars represent the mean \pm standard error of the mean. Results were considered significant if $p < 0.05$.

RESULTS

Expression of ABCA4 with AAV dual vectors

The well-established genotype/autofluorescence phenotype relationship makes autosomal recessive ABCA4 Stargardt disease a prototypical target to validate the feasibility of an AAV dual vector-mediated gene therapy. We, therefore, cloned the 6.8 kb coding sequence of human ABCA4 into a vector plasmid under the control of a strong ubiquitous cytomegalovirus/chicken β -actin (smCBA) promoter and followed it by a bovine growth hormone polyA (Fig. 1A). The overlap vectors then constructed share a 1.35 kb internal overlap sequence between 5' and 3' vector genomes (B1–B3 in Fig. 1) and provide a target for recombination to occur. To create the transplicing dual vectors (Fig. 1C), the coding sequence was split at the exon21/22 splice junction, making the 3' end of exon21 the end of the front half vector and the 5' end of exon22 the start of the back half vector. The natural splicing signals were replaced with consensus splice donor/acceptor sites. However, transplicing-only vectors must rely solely on the random interaction of the ITRs for homologous recombination or nonhomologous end joining. Therefore, overlap and transplicing approaches were also combined in the hybrid dual vector system (Fig. 1D) that, in addition to the splice donor/acceptor sites, contain a short overlapping sequence known to facilitate high frequency *in vivo* recombination with improved recombination directionality.⁴²

ABCA4 dual vector platforms were constructed as diagramed and packaged into AAV2 for *in vitro* evaluation. Infection of HEK293 cells with overlap, transplicing, and hybrid dual vector platforms at an MOI of 10,000 of each vector revealed that ABCA4 is expressed and migrates at the same molecular weight as the transfection control of a plasmid containing the complete coding sequence of ABCA4 (Fig. 2). This confirms that when the full-length coding sequence split between dual vectors, it can be reconstituted to express the full-length protein when delivered to cells *in vitro*. All dual vector platforms expressed detectable levels of full-length ABCA4 with the hybrid platform clearly exhibiting the strongest expression followed by the transplicing platform, which produced only \sim 50% of that seen with the hybrid platform. In contrast, the overlap platforms tested did express ABCA4, however, at levels only barely above the detection minimum.

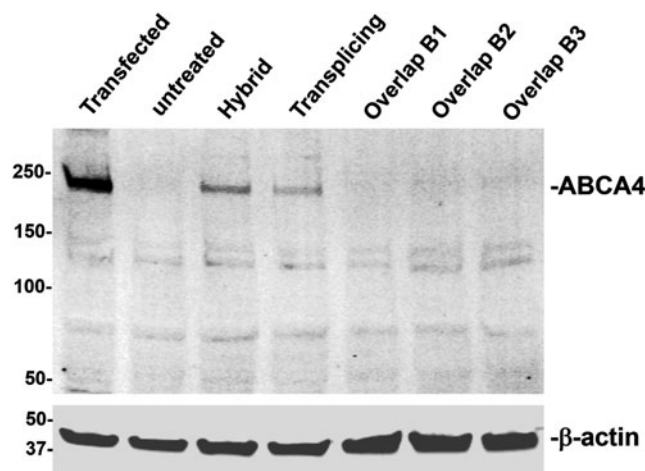


Figure 2. Western blot comparison of the expression efficiency of ABCA4 dual vector platforms. HEK293 cells were transfected with plasmid containing full-length ABCA4 (left lane) or infected with ABCA4 dual vectors as indicated packaged in AAV2 at an MOI of 10,000 vector genomes per cell of each vector. HEK293, human embryonic kidney; MOI, multiplicity of infection.

Evaluation of ABCA4 expression in an ABCA4^{-/-} mouse model

The best performing dual vector platform from the *in vitro* experiments, the AAV hybrid system, was then repackaged into AAV8(Y733F), an efficient serotype for transduction of photoreceptors,⁴⁹ and analyzed *in vivo* (Fig. 3). ABCA4^{-/-} mice were subretinally injected into one eye with 3×10^9 total vector genomes per eye ($1 \mu\text{L}$ of 3×10^{12} vg/mL) at 4 weeks of age. Four weeks postinjection, the mice were euthanized and the retinas were extracted for Western blotting (Fig. 3A) or whole eye cups were prepared for sectioning and immunohistochemistry (Fig. 3B, C). As a negative control, a 5' half vector only was injected separately. Immunoblots stained with rim5B4, an antibody against the N-half of the protein, revealed that ABCA4 is expressed in knockout (KO) mice after treatment with hybrid dual AAV vectors. The relative amount of ABCA4 protein is <20% of the levels present in a C57BL/6 wild-type mouse. Critically, immunohistochemical evaluation of treated retinal sections of KO mice revealed that ABCA4 protein delivered by dual AAV vectors localizes properly to its endogenous location in photoreceptor outer segments.

RNA from retinas of mice injected with the ABCA4 hybrid vector was extracted and the region containing the splice donor and acceptor sites in the 5' and 3' vectors from multiple independently isolated clones was analyzed by sequencing (Supplementary Fig. S1). Their perfect alignment relative to the ABCA4 reference wild-type sequence demonstrates that splicing of the pre-

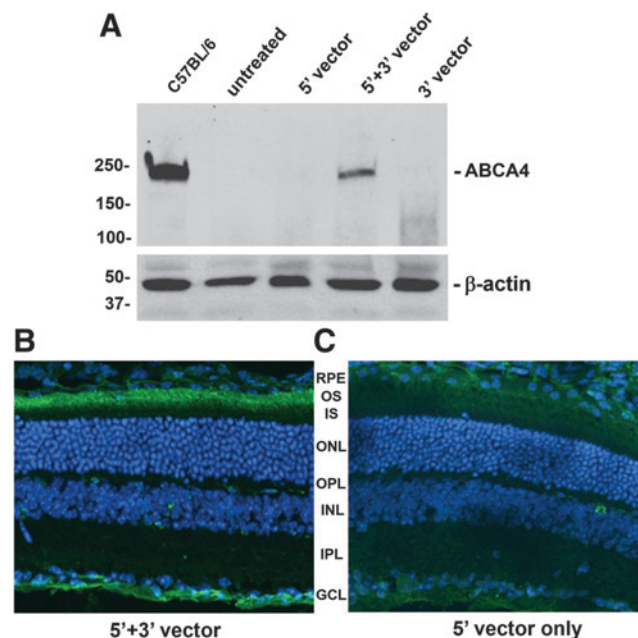


Figure 3. The most efficient ABCA4 dual vector system, based on the *in vitro* studies mentioned, the hybrid system, was repackaged in AAV8(Y733F) and subretinally injected into 1-month-old ABCA4^{-/-} mice with $1 \mu\text{L}$ of 3×10^9 vg/mL of each half vector, and protein expression was then analyzed 4 weeks after injection by Western blot (A) or immunohistochemistry (B, C) with specific antibodies against the N-terminal (rim5B4) half of human ABCA4. As a control, the front half vector (5' vector) only was injected (A, C) in some animals. GCL, retinal ganglion cell layer; INL, inner nuclear layer; IPL, inner plexiform layer; IS, inner segments; ONL, outer nuclear layer; OPL, outer plexiform layer; OS, outer segments; RPE, retinal pigment epithelium.

mRNA of concatemerized 5' and 3' vectors in the dual hybrid vector system occurs with high fidelity and specificity.

Autofluorescence and A2E accumulation in hybrid dual vector-treated ABCA4^{-/-} mice

A2E is the major fluorescent compound of pisciform lipofuscin aggregates in human patients.¹³ ABCA4^{-/-} mice also exhibit an increase of 488 nm autofluorescence with age due to the accumulation of A2E in the RPE.⁵³ This accumulation of lipofuscin/A2E autofluorescence was measured at monthly intervals with a cSLO up to 5 months postinjection (Fig. 4). Animals treated with the hybrid dual vector platform consisting of a 1:1 mixture of 5' and 3' vectors showed significantly reduced lipofuscin/A2E levels relative to the contralateral eye that was left untreated (Fig. 4). This was not observed in animals treated with the 5' vector alone, confirming that A2E reduction required expression of functional full-length ABCA4 from the hybrid vector. The amount of A2E present in vector-treated and untreated retinas at various times post-treatment as determined by HPLC is

shown Fig. 5 and confirms that A2E is significantly reduced in hybrid dual vector-treated eyes.

In vivo anatomic integrity of the retinal outer nuclear layer was confirmed by optical coherence tomography at 5 months of age (Supplementary Fig. S2). Treated retinas showed only minor thinning of the outer nuclear layer consistent with the minor photoreceptor loss typically associated with transient retinal detachments caused by vector subretinal injection as well as damage in the periphery surrounding the injection retinotomy.⁵⁸

DISCUSSION

AAV vector-mediated somatic gene therapy has had demonstrated success in multiple animal models and clinical trials of retinal degenerations, and recently the first clinical use of AAV-based retinal gene therapy was approved by the FDA.^{14–16,18,22,51,59} The ability to deliver transgenes beyond the DNA size packaging limits of a single AAV vector would increase AAV-based vector utility as a more general gene delivery vehicle considerably. In this article, we compared the capacity of different AAV dual vector systems to deliver an oversized ABCA4 transgene *in vitro* and present the effect of AAV hybrid dual vector delivered ABCA4 on A2E bisretinoid formation *in vivo*.

Despite the inherent inefficiency of dual AAV vectors compared with single AAV vectors,⁶⁰ it was reported that a variety of AAV dual vector systems can produce measurable amounts of protein and exhibit a therapeutic effect,^{25,36,37,61,62} and three of these systems for expressing full-length protein from large cDNAs are evaluated here. McClements *et al.* recently showed in a mouse model of ABCA4 Stargardt disease that an optimized dual vector overlap system has a significant effect on lowering bisretinoid levels.²⁵ The AAV8Y733F serotype employed here is highly efficient for the transduction of photoreceptor cells⁴⁹ and was used both in McClements *et al.* and in this study. Those authors also reported that the total amount of ABCA4 protein produced by their optimized overlap system is only ~1% of the wild-type levels. This is in accordance with our findings (Fig. 2) that three overlap systems of different overlap lengths produce protein *in vitro* barely above the detection minimum. The overlap lengths for our overlap vector systems B2 and B3 (Fig. 1) were chosen based on unique restriction sites within the ABCA4 sequence. Their expression of full-length ABCA4 protein appears to be similar in magnitude to the suboptimal overlap systems described by McClements *et al.*²⁵ In addition, the length of dual vector overlaps appear to be limited in the degree to which

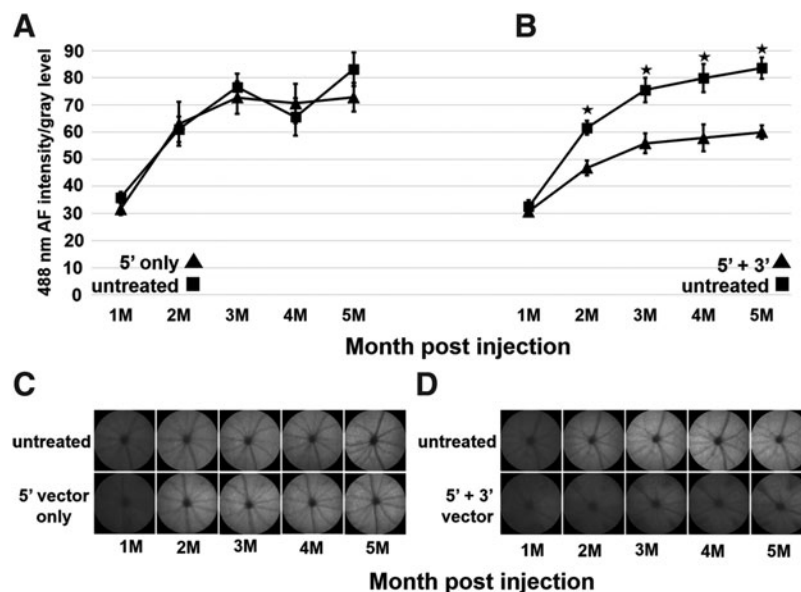


Figure 4. FAF quantification of lipofuscin/A2E accumulation of ABCA4 hybrid dual vector-treated and untreated ABCA4^{-/-} mouse retinas. AAV hybrid dual vectors packaged in AAV8(Y733F) were subretinally injected at 1 month of age. One eye was injected while the contralateral eye was left untreated. Autofluorescence was measured with a Heidelberg Engineering cSLO HRA+OCT at monthly intervals after injection. **(A, B)** quantification of FAF as a function of months after vector treatment. **(C, D)** examples of FAF images from which the data in **(A, B)** were derived. **(A, C)** FAF of ABCA4^{-/-} animals treated with the 5' vector only. **(B, D)** FAF in 5' plus 3' dual vector-treated animals. Error bars represent the mean ± SEM. ★ $p < 0.05$. A2E, N-retinylidene-N-retinylethanolamine; cSLO, confocal scanning laser ophthalmoscope; FAF, fundus autofluorescence; HRA, Heidelberg retinal angiograph; OCT, optical coherence tomography; SEM, standard error of the mean.

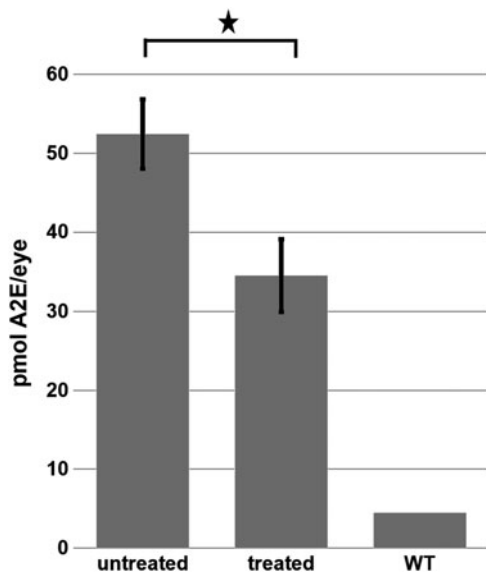


Figure 5. Quantification of A2E in the retinas of untreated and ABCA4 hybrid dual vector-treated ABCA4^{-/-} mice as measured by HPLC. Retinas were examined 5 months after vector treatment. Error bars represent the mean ± SEM. ★*p* < 0.05. HPLC, high-performance liquid chromatography.

they can be optimized. Although it was shown that the overlap does not have to be large for ABCA4,²⁵ probably because it contains a motif facilitating efficient recombination within the overlap region, this might not be true for other cDNAs. It might also be the case that a region facilitating efficient recombination cannot always be found in the area of the cDNA that can be used for the dual vector overlap, which is usually limited to the central region of the sequence.

Second, it is important to appreciate that the cellular DNA damage repair mechanism leading to reconstitution of the full-length sequence from simple overlap dual vectors must be a homologous recombination, and homologous recombination is downregulated in terminally differentiated cells such as photoreceptors. Therefore, the predominant repair mechanism in photoreceptor cells is nonhomologous end joining,⁶³ a process that may lead to incorrect joining of two simple overlap dual vectors.

The AAV dual vector hybrid system employed here and shown to be the most efficient at expressing full-length ABCA4 is independent of the DNA damage response mechanism for reconstitution of the full-length sequence. Its superiority over the simple overlap dual vector system might explain the much higher full-length protein production observed here, which reaches ~10% of wild-type levels. Interestingly, McClements *et al.* injected about 3.3 times more vector genome copies per eye than was used in our experiments.²⁵ This suggests

that an increase in hybrid dual vector genome copies per eye might further increase the efficiency of the AAV hybrid dual vector system to levels even closer to wild-type levels.

The increase of autofluorescence due to accumulation of bisretinoids is often used as the primary diagnostic tool for the early clinical evaluation of Stargardt disease.^{13,64} The available rodent models for ABCA4 Stargardt disease also show an increase in autofluorescence with age. However, in human Stargardt disease, this fluorescence is initially visible as small, fish-shaped, or pisciform autofluorescent foci surrounding the central fovea,^{13,64} whereas in mice it is seen as a generally uniform autofluorescence across the entire retina (Fig. 4).⁵³ Clearly the differences in the cone-rod distribution between their concentric organization in the human retina as compared with their relatively uniform distribution with eccentricity in the mouse retina may play a defining role in these phenotypic pattern differences in ABCA4-mediated autofluorescence. However, as the majority of the A2E accumulated is localized in the RPE, it remains unclear why autofluorescence in the mutant ABCA4 mouse exhibits a more uniform pattern than that seen in the human.

Previous studies showed that AAV dual vector ABCA4 treatment reduces the accumulation of toxic bisretinoids.²⁵ Other AAV dual vector approaches³⁷ and nanoparticle delivery⁶⁵ have also demonstrated that recombinant ABCA4 expression leads to a reduction of lipofuscin granules in the RPE. We present here for the first time *in vivo* data that AAV hybrid dual vector expressed ABCA4 reduces the autofluorescence phenotype caused by A2E/lipofuscin accumulation and demonstrate that this effect persists for at least 5 months post-treatment (Figs. 4 and 5).

Overall, the results of our study suggest that the supplementation of a functional form of ABCA4 protein delivered with hybrid dual AAV vectors can significantly reduce A2E accumulation in the ABCA4^{-/-} animal model of Stargardt disease, supporting its further development as a viable gene therapy option for the corresponding human condition.

ACKNOWLEDGMENTS

The authors thank Dr. Seok-Hong Min and Dr. Ping Zhu for their excellent technical assistance.

AUTHOR DISCLOSURE

The University of Florida and W.W.H. have a financial interest in the use of AAV therapies, and W.W.H. owns equity in a company (AGTC) that

might in the future commercialize some aspects of this work. F.M.D., L.L.M., V.A.C., and R.S.M. declare no conflicts of interest.

FUNDING INFORMATION

W.W.H. and F.M.D. received research funding from AGTC for this project. This study was also funded, in part, by grants from the National In-

stitutes of Health (Grant No. EY002422) and Canadian Institutes of Health Research (Grant No. PJT 148649) to R.S.M.

SUPPLEMENTARY MATERIAL

Supplementary Figure S1

Supplementary Figure S2

REFERENCES

- Blacharski PA. Fundus flavimaculatus. In: Newsome DA, ed. *Retinal Dystrophies and Degenerations*. New York: Raven Press, 1988:135–159.
- Allikmets R. A photoreceptor cell-specific ATP-binding transporter gene (ABCR) is mutated in recessive Stargardt macular dystrophy. *Nat Genet* 1997;17:122.
- Sun H, Nathans J. Stargardt's ABCR is localized to the disc membrane of retinal rod outer segments. *Nat Genet* 1997;17:15–16.
- Lenis TL, Hu J, Ng SY, et al. Expression of ABCA4 in the retinal pigment epithelium and its implications for Stargardt macular degeneration. *Proc Natl Acad Sci U S A* 2018;115:E11120–E11127.
- Illing M, Molday LL, Molday RS. The 220-kDa rim protein of retinal rod outer segments is a member of the ABC transporter superfamily. *J Biol Chem* 1997;272:10303–10310.
- Molday LL, Wahl D, Sarunic MV, et al. Localization and functional characterization of the p.Asn965Ser (N965S) ABCA4 variant in mice reveal pathogenic mechanisms underlying Stargardt macular degeneration. *Hum Mol Genet* 2018;27:295–306.
- Bungert S, Molday LL, Molday RS. Membrane topology of the ATP binding cassette transporter ABCR and its relationship to ABC1 and related ABCA transporters: identification of N-linked glycosylation sites. *J Biol Chem* 2001;276:23539–23546.
- Molday RS, Beharry S, Ahn J, et al. Binding of N-retinylidene-PE to ABCA4 and a model for its transport across membranes. *Adv Exp Med Biol* 2006;572:465–470.
- Chen C, Thompson DA, Koutalos Y. Reduction of all-trans-retinal in vertebrate rod photoreceptors requires the combined action of RDH8 and RDH12. *J Biol Chem* 2012;287:24662–24670.
- Radu RA, Mata NL, Bagla A, et al. Light exposure stimulates formation of A2E oxiranes in a mouse model of Stargardt's macular degeneration. *Proc Natl Acad Sci U S A* 2004;101:5928–5933.
- Radu RA, Yuan Q, Hu J, et al. Accelerated accumulation of lipofuscin pigments in the RPE of a mouse model for ABCA4-mediated retinal dystrophies following Vitamin A supplementation. *Invest Ophthalmol Vis Sci* 2008;49:3821–3829.
- Mata NL, Weng J, Travis GH. Biosynthesis of a major lipofuscin fluorophore in mice and humans with ABCR-mediated retinal and macular degeneration. *Proc Natl Acad Sci U S A* 2000;97:7154–7159.
- Fishman GA, Stone EM, Grover S, et al. Variation of clinical expression in patients with Stargardt dystrophy and sequence variations in the ABCR gene. *Arch Ophthalmol* 1999;117:504–510.
- Constable IJ, Pierce CM, Lai CM, et al. Phase 2a randomized clinical trial: safety and post hoc analysis of subretinal rAAV.sFLT-1 for wet age-related macular degeneration. *EBioMedicine* 2016;14:168–175.
- Bennett J, Wellman J, Marshall KA, et al. Safety and durability of effect of contralateral-eye administration of AAV2 gene therapy in patients with childhood-onset blindness caused by RPE65 mutations: a follow-on phase 1 trial. *Lancet* 2016;388:661–672.
- Ghazi NG, Abboud EB, Nowilaty SR, et al. Treatment of retinitis pigmentosa due to MERTK mutations by ocular subretinal injection of adeno-associated virus gene vector: results of a phase I trial. *Hum Genet* 2016;135:327–343.
- Pierce EA, Bennett J. The status of RPE65 gene therapy trials: safety and efficacy. *Cold Spring Harb Perspect Med* 2015;5:a017285.
- Cideciyan AV, Hauswirth WW, Aleman TS, et al. Human RPE65 gene therapy for Leber congenital amaurosis: persistence of early visual improvements and safety at 1 year. *Hum Gene Ther* 2009;20:999–1004.
- Nathwani AC, Tuddenham EG, Rangarajan S, et al. Adenovirus-associated virus vector-mediated gene transfer in hemophilia B. *N Engl J Med* 2011;365:2357–2365.
- Bowles DE, McPhee SW, Li C, et al. Phase 1 gene therapy for Duchenne muscular dystrophy using a translational optimized AAV vector. *Mol Ther* 2012;20:443–455.
- Flotte TR, Trapnell BC, Humphries M, et al. Phase 2 clinical trial of a recombinant adeno-associated viral vector expressing alpha1-antitrypsin: interim results. *Hum Gene Ther* 2011;22:1239–1247.
- Bainbridge JW, Smith AJ, Barker SS, et al. Effect of gene therapy on visual function in Leber's congenital amaurosis. *N Engl J Med* 2008;358:2231–2239.
- Simonelli F, Maguire AM, Testa F, et al. Gene therapy for Leber's congenital amaurosis is safe and effective through 1.5 years after vector administration. *Mol Ther* 2010;18:643–650.
- Hauswirth WW, Aleman TS, Kaushal S, et al. Treatment of leber congenital amaurosis due to RPE65 mutations by ocular subretinal injection of adeno-associated virus gene vector: short-term results of a phase I trial. *Hum Gene Ther* 2008;19:979–990.
- McClements ME, Barnard AR, Singh MS, et al. An AAV dual vector strategy ameliorates the Stargardt phenotype in adult *Abca4*($-/-$) mice. *Hum Gene Ther* 2019;30:590–600.
- Voretigene neparvovec-rzyl (Luxturna) for inherited retinal dystrophy. *Med Lett Drugs Ther* 2018;60:53–55.
- Allocca M, Doria M, Petrillo M, et al. Serotype-dependent packaging of large genes in adeno-associated viral vectors results in effective gene delivery in mice. *J Clin Invest* 2008;118:1955–1964.
- Dong B, Nakai H, Xiao W. Characterization of genome integrity for oversized recombinant AAV vector. *Mol Ther* 2010;18:87–92.
- Lai Y, Yue Y, Duan D. Evidence for the failure of adeno-associated virus serotype 5 to package a viral genome $> or = 8.2$ kb. *Mol Ther* 2010;18:75–79.
- Wu Z, Yang H, Colosi P. Effect of genome size on AAV vector packaging. *Mol Ther* 2010;18:80–86.
- Kapranov P, Chen L, Dederich D, et al. Native molecular state of adeno-associated viral vectors revealed by single-molecule sequencing. *Hum Gene Ther* 2012;23:46–55.
- Hirsch ML, Li C, Bellon I, et al. Oversized AAV transduction is mediated via a DNA-PKcs-independent, Rad51C-dependent repair pathway. *Mol Ther* 2013;21:2205–2216.

33. McClements ME, Charbel Issa P, Blouin V, et al. A fragmented adeno-associated viral dual vector strategy for treatment of diseases caused by mutations in large genes leads to expression of hybrid transcripts. *J Genet Syndr Gene Ther* 2016;7:311.
34. Yan Z, Ritchie TC, Duan D, et al. Recombinant AAV-mediated gene delivery using dual vector heterodimerization. *Methods Enzymol* 2002;346:334–357.
35. Ghosh A, Yue Y, Lai Y, et al. A hybrid vector system expands adeno-associated viral vector packaging capacity in a transgene-independent manner. *Mol Ther* 2008;16:124–130.
36. Dyka FM, Boye SL, Chiodo VA, et al. Dual adeno-associated virus vectors result in efficient in vitro and in vivo expression of an oversized gene, MYO7A. *Hum Gene Ther Meth* 2014;25:166–177.
37. Lopes VS, Boye SE, Louie CM, et al. Retinal gene therapy with a large MYO7A cDNA using adeno-associated virus. *Gene Ther* 2013;20:824–833.
38. Barnard AR, Groppe M, MacLaren RE. Gene therapy for choroideremia using an adeno-associated viral (AAV) vector. *Cold Spring Harb Perspect Med* 2014;5:a017293.
39. Blankinship MJ, Gregorevic P, Allen JM, et al. Efficient transduction of skeletal muscle using vectors based on adeno-associated virus serotype 6. *Mol Ther* 2004;10:671–678.
40. Colella P, Trapani I, Cesi G, et al. Efficient gene delivery to the cone-enriched pig retina by dual AAV vectors. *Gene Ther* 2014;21:450–456.
41. Trapani I, Colella P, Sommella A, et al. Effective delivery of large genes to the retina by dual AAV vectors. *EMBO Mol Med* 2014;6:194–211.
42. Ghosh A, Yue Y, Duan D. Efficient transgene reconstitution with hybrid dual AAV vectors carrying the minimized bridging sequences. *Hum Gene Ther* 2011;22:77–83.
43. Yan Z, Lei-Butters DC, Zhang Y, et al. Hybrid adeno-associated virus bearing nonhomologous inverted terminal repeats enhances dual-vector reconstruction of minigenes in vivo. *Hum Gene Ther* 2007;18:81–87.
44. Duan D, Yue Y, Engelhardt JF. Expanding AAV packaging capacity with trans-splicing or overlapping vectors: a quantitative comparison. *Mol Ther* 2001;4:383–391.
45. Duan D, Yue Y, Yan Z, et al. Trans-splicing vectors expand the packaging limits of adeno-associated virus for gene therapy applications. *Methods Mol Med* 2003;76:287–307.
46. Lai Y, Yue Y, Liu M, et al. Synthetic intron improves transduction efficiency of trans-splicing adeno-associated viral vectors. *Hum Gene Ther* 2006;17:1036–1042.
47. Hirsch ML, Storici F, Li C, et al. AAV recombineering with single strand oligonucleotides. *PLoS One* 2009;4:e7705.
48. Lostal W, Kodippili K, Yue Y, et al. Full-length dystrophin reconstitution with adeno-associated viral vectors. *Hum Gene Ther* 2014;25:552–562.
49. Petrs-Silva H, Dinculescu A, Li Q, et al. High-efficiency transduction of the mouse retina by tyrosine-mutant AAV serotype vectors. *Mol Ther* 2009;17:463–471.
50. Zolotukhin S, Potter M, Zolotukhin I, et al. Production and purification of serotype 1, 2, and 5 recombinant adeno-associated viral vectors. *Methods* 2002;28:158–167.
51. Jacobson SG, Acland GM, Aguirre GD, et al. Safety of recombinant adeno-associated virus type 2-RPE65 vector delivered by ocular subretinal injection. *Mol Ther* 2006;13:1074–1084.
52. Timmers AM, Zhang H, Squitieri A, et al. Subretinal injections in rodent eyes: effects on electrophysiology and histology of rat retina. *Mol Vis* 2001;7:131–137.
53. Charbel Issa P, Barnard AR, Singh MS, et al. Fundus autofluorescence in the *Abca4*($-/-$) mouse model of Stargardt disease—correlation with accumulation of A2E, retinal function, and histology. *Invest Ophthalmol Vis Sci* 2013;54:5602–5612.
54. Kim SR, Fishkin N, Kong J, et al. Rpe65 Leu450-Met variant is associated with reduced levels of the retinal pigment epithelium lipofuscin fluorophores A2E and iso-A2E. *Proc Natl Acad Sci U S A* 2004;101:11668–11672.
55. Quazi F, Molday RS. ATP-binding cassette transporter ABCA4 and chemical isomerization protect photoreceptor cells from the toxic accumulation of excess 11-cis-retinal. *Proc Natl Acad Sci U S A* 2014;111:5024–5029.
56. Molday LL, Rabin AR, Molday RS. ABCR expression in foveal cone photoreceptors and its role in Stargardt macular dystrophy. *Nat Genet* 2000;25:257–258.
57. Cheng CL, Djajadi H, Molday RS. Cell-specific markers for the identification of retinal cells by immunofluorescence microscopy. *Methods Mol Biol* 2013;935:185–199.
58. Matsumoto H, Kataoka K, Tsoka P, et al. Strain difference in photoreceptor cell death after retinal detachment in mice. *Invest Ophthalmol Vis Sci* 2014;55:4165–4174.
59. Acland GM, Aguirre GD, Ray J, et al. Gene therapy restores vision in a canine model of childhood blindness. *Nat Genet* 2001;28:92–95.
60. Carvalho LS, Turunen HT, Wassmer SJ, et al. Evaluating efficiencies of dual AAV approaches for retinal targeting. *Front Neurosci* 2017;11:503.
61. Akil O, Dyka F, Calvet C, et al. Dual AAV-mediated gene therapy restores hearing in a DFNB9 mouse model. *Proc Natl Acad Sci U S A* 2019 [Epub ahead of print]; DOI: 10.1073/pnas.1817537116.
62. Kodippili K, Hakim CH, Pan X, et al. Dual AAV gene therapy for duchenne muscular dystrophy with a 7-kb mini-dystrophin gene in the canine model. *Hum Gene Ther* 2018;29:299–311.
63. Frohns A, Frohns F, Naumann SC, et al. Inefficient double-strand break repair in murine rod photoreceptors with inverted heterochromatin organization. *Curr Biol* 2014;24:1080–1090.
64. Burke TR, Duncker T, Woods RL, et al. Quantitative fundus autofluorescence in recessive Stargardt disease. *Invest Ophthalmol Vis Sci* 2014;55:2841–2852.
65. Han Z, Conley SM, Makkia RS, et al. DNA nanoparticle-mediated ABCA4 delivery rescues Stargardt dystrophy in mice. *J Clin Invest* 2012;122:3221–3226.

Received for publication June 3, 2019;
accepted after revision August 9, 2019.

Published online: August 15, 2019.